Metal Dependency for Transcription Factor Rho Activation†

Thomas P. Weber,‡ William R. Widger,§ and Harold Kohn*,||

Department of Chemistry, University of Houston, Houston Texas 77204-5641, Department of Biology and Biochemistry, University of Houston, Houston, Texas 77204-5934, and Division of Medicinal Chemistry and Natural Products, School of Pharmacy, University of North Carolina, Chapel Hill, North Carolina 27599-7360

Received September 26, 2002

ABSTRACT: The *Escherichia coli* rho transcription termination factor terminates select transcripts and rho activity requires Mg^{2+}. We investigated whether divalent metal ions other than Mg^{2+} catalyze rho-dependent ATP hydrolysis to ADP and P_i in vitro. The effects of 11 divalent metal ions (Be^{2+}, Ca^{2+}, Cd^{2+}, Co^{2+}, Cu^{2+}, Hg^{2+}, Mn^{2+}, Ni^{2+}, Sr^{2+}, VO^{2+}, Zn^{2+}) on ATPase activity were determined in the absence and presence of $MgCl_2$. Without $MgCl_2$, Ca^{2+}, Cd^{2+}, Co^{2+}, Cu^{2+}, Hg^{2+}, Mn^{2+}, Ni^{2+}, VO^{2+}, and Zn^{2+} activated ATP hydrolysis with either hyberbolic (Ca^{2+}, Co^{2+}, Cu^{2+}, Hg^{2+}, VO^{2+}), peak velocity (Cd^{2+}, Mn^{2+}, Zn^{2+}), or sigmoidal (Ni^{2+}) rate acceleration curves. Sr^{2+} was found to be a nonactivator and Be^{2+} an inhibitor of rho-dependent ATPase activity. The metals' effects were compared with Mg^{2+} and gave different rank orders when either the velocity (V_{max}, V_{peak}) or the efficiency (V_{max}/K_M, V_{peak}/K_M) of ATP hydrolysis was used as the determinant (V: $Mg^{2+} \sim Mn^{2+} > Zn^{2+} > Co^{2+} > Ni^{2+} \sim Cd^{2+} > Ca^{2+} > Cu^{2+} > Hg^{2+} \sim VO^{2+}$; V/K_M: $Mg^{2+} > Mn^{2+} > Ca^{2+} > Co^{2+} > Zn^{2+} > Cu^{2+} > Ni^{2+} > Hg^{2+} > Cd^{2+}$). Mg^{2+} proved to be the most effective divalent metal. We observed that the metal-dependent rates were affected by metal ion interactions with rho, RNA, and the buffer constituents. Significantly, replacement of the octahedral Mg^{2+} ion by metals that typically prefer coordination spheres less than six (Cd^{2+}, Co^{2+}, Ni^{2+}, VO^{2+}, Zn^{2+}) led to ATPase activity, suggesting that the putative $Mg{\cdot}ATP^{2-}$ coordination sphere in rho does not need to remain fully intact for ATP hydrolysis.

The *Escherichia coli* rho factor rho (*1*) is composed of six identical 47-kDa proteins of 419 amino acids (*2*). Rho terminates transcripts synthesized by RNA polymerase at specific sites on DNA templates (*3*, *4*). A tethered tracking mechanism has been proposed for enzyme function whereby rho advances along the nascent RNA in a process fueled by ATP[1] hydrolysis and leads to the disruption of the RNA polymerase−transcription complex and release of the transcript (*3*, *4*). The essential nature of the rho factor in Gram-negative bacterial processes has been demonstrated through the use of temperature-sensitive *E. coli* mutants in rho (*5*−*7*) and the introduction of an inactivated plasmid copy of rho into the genome (*8*).

Mg^{2+} is necessary for rho-mediated ATPase activity. In the absence of Mg^{2+}, no ATP hydrolysis occurs (*9*, *10*). We have shown that Mg^{2+} functions as a nonessential activator where $Mg{\cdot}ATP^{2-}$ is the likely substrate for ATP hydrolysis and a second Mg^{2+} is required for maximal ATP hydrolysis (*11*).

Mg^{2+} is the predominant metal cofactor in *E. coli* metal-dependent ATPases (*12*). Studies have also demonstrated that Mg^{2+} can be replaced in vitro to provide ATPases of varying efficiencies (*13*−*17*). Selective substitution of the metal cofactor by other metals provides information on the electronic, structural, and catalytic requirements necessary for enzymatic processes similar to insights learned from site-specific mutagenesis and substrate structure−activity studies. We show in this investigation that rho supports other divalent metals but that their efficiencies for ATP hydrolysis depends on their concentrations and their interactions with biological macromolecules and the reaction constituents.

METHODS AND MATERIALS

Materials. Bicyclomycin was a gift from Fujisawa Pharmaceutical Co., Ltd., and was purified by three successive silica gel chromatographies using 20% methanol-chloroform as the eluant. [γ-^{32}P] ATP (6000 Ci/mmol) was purchased from Perkin-Elmer (Boston, MA), Bio-Spin 6 columns were from Bio-Rad (Hercules, CA), and PEI-TLC plates used for ATPase assays were obtained from J. T. Baker, Inc. (Phillipsburg, NJ). SDS−PAGE was performed using the Xcell *SureLock* apparatus, and NuPage Novex 4−12% Bis-Tris gels and MOPS SDS Running Buffer (20x) were obtained from Invitrogen (Carlsbad, CA). Poly(C) was from Sigma (St. Louis, MO) and was dissolved in 100 μL of TE buffer and dialyzed against aqueous 1.0 M potassium phosphate, pH 7.0 (8 h, 2×, 4 °C), using Slide-A-Lyzer cassettes from Pierce (Rockford, IL). All other chemicals

† This work was supported by the National Institutes of Health Grant GM37934 and the Robert A. Welch Foundation Grant E1381 (W.R.W.).

* To whom all correspondence should be addressed. Email: harold_kohn@unc.edu.

‡ Department of Chemistry, University of Houston.

§ Department of Biology and Biochemistry, University of Houston.

|| University of North Carolina.

[1] Abbreviations: ATP, adenosine 5′-triphosphate; DTT, dithiothreitol; EDTA, ethylenediaminetetraacetic acid; PEI-TLC, poly(ethyleneimine) thin-layer chromatography; SDS−PAGE, sodium dodecyl sulfate-polyacrylamide gel electrophoresis; TE, Tris·HCl and EDTA; Tris, tris-(hydroxymethyl)aminomethane.

10.1021/bi020601y CCC: $25.00
Published on Web 01/14/2003

were reagent grade. All metals salts ($MgCl_2$, $BeCl_2$, $CaCl_2$, $CdCl_2$, $CoCl_2$, $CuSO_4$, $Hg(OAc)_2$, $MnCl_2$, $NiCl_2$, $SrCl_2$, $VOSO_4$, $ZnCl_2$) were purchased from Sigma-Aldrich (St. Louis, MO) and were the highest grade available.

Bacterial Strains and Plasmids. Wild-type rho from *E. coli* was purified as described by Mott (*18*) from strain AR120 containing plasmid p39-ASE (*19*). Rho purity was determined by SDS−PAGE, and protein concentration was measured according to the Lowry assay (*20*).

Removal of Endogenous Mg^{2+} from Rho. Rho treatment was carried out as previously described (*11*).

Poly(C)-Dependent ATPase Assay (21) for Rho Activation by Divalent Metal Ions. The Mg^{2+}-free rho (spin column purified) ribonucleotide-stimulated ATPase activity at 32 °C was assayed as follows. Reactions were initiated by adding ATP (200 μM) and 0.5 μCi [γ-^{32}P] ATP to the solution containing 40 mM Tris·HCl (pH 7.9), 50 mM KCl, 100 nM (unless otherwise indicated) poly(C), 100 nM (unless otherwise indicated) rho (monomer), and one of the following salts: $MgCl_2$, $BeCl_2$, $CaCl_2$, $CdCl_2$, $CoCl_2$, $CuSO_4$, $Hg(OAc)_2$, $MnCl_2$, $NiCl_2$, $SrCl_2$ $VOSO_4$, or $ZnCl_2$, (0−4 mM). Aliquots (1.4 μL, 5×) were spotted every 15 s on PEI-TLC plates and chromatographed. The amount of ^{32}P-labeled inorganic phosphate hydrolyzed from ATP after separation on PEI-TLC plates (prerun with water and dried) using 0.75 M potassium phosphate (pH 3.5) as the mobile phase was measured by exposure to PhosphorImager plates (Fuji and Molecular Dynamics) (1−4 h), scanned on a Storm 860 PC PhosphorImager, and analyzed using Molecular Dynamic's ImageQuant 5.0 software. The initial rates of the reactions were determined by plotting the amount of ATP hydrolyzed against time. Each reaction was performed in duplicate, and the results were averaged.

Poly(C)-Dependent ATPase Assay for Rho Activation by Divalent Metal Ions in the Presence of $MgCl_2$. Reactions were initiated by adding ATP (200 μM) and 0.5 μCi [γ-^{32}P] ATP to the solution containing 40 mM Tris·HCl (pH 7.9), 50 mM KCl, 100−250 nM poly(C), 100−250 nM nonspin column-treated rho (monomer), $MgCl_2$ (1 or 10 mM), and 0−4 mM of one of the following salts: $BeCl_2$, $CaCl_2$, $CdCl_2$, $CoCl_2$, $CuSO_4$, $Hg(OAc)_2$, $NiCl_2$, $SrCl_2$, $VOSO_4$, or $ZnCl_2$. The reactions were analyzed as described above.

Poly(C)-Dependent ATPase Assays for Rho in the Presence of Bicyclomycin (**1**). The inhibition of ribonucleotide-stimulated ATPase activity of Mg^{2+}-depleted rho in the presence of either $MgCl_2$, $MnCl_2$, or $ZnCl_2$ was measured at 32 °C using a six-channel, multiwell procedure (*11*). Reactions were initiated by mixing 200 μM ATP containing 0.5 μCi [γ-^{32}P] ATP to a solution containing 40 mM Tris·HCl (pH 7.9), 50 mM KCl, 100 nM poly(C), 100 nM rho (monomer), using either $MgCl_2$ (200 μM) or $MnCl_2$ (200 μM) or $ZnCl_2$ (100 μM) as the divalent metal source, and **1** concentrations ranging from 0 to 400 μM. The reactions were analyzed as described above.

RESULTS

We envisioned numerous pathways by which metals could affect rho-mediated poly(C)-dependent ATP hydrolysis. The metal ion may assist ATP binding, catalyze ATP hydrolysis, and chaperone ATP and ADP from the hydrolysis site.

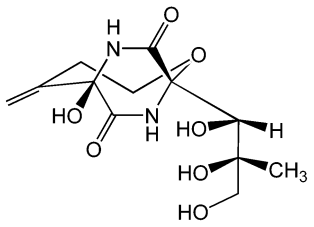

1

Alternatively, the metals may adversely interact with either rho, poly(C), or ATP and prevent rho-mediated ATP hydrolysis.

The potential metal-dependent profiles can be grouped into the four patterns previously predicted by London and Steck (*22*). First are hyperbolic metal activation curves. These curves show Michaelis−Menten kinetics and contain one V_{max} and one K_M value for the substrate $M{\cdot}ATP^{2-}$, where M^{2+} can be any divalent cation. Second are metal activation curves that increase with increasing metal concentration and then decrease as the metal concentrations further increase. These velocity curves exhibit a peak velocity, V_{peak}. Third are activation curves that show a sigmoidal shape for the ATP hydrolysis rate versus total M^{2+} concentration. The sigmoidal shape provides information about cooperative processes for ATP hydrolysis where metal binding at one site either enhances or diminishes ATP hydrolysis at another site. However, care must be taken when interpreting sigmoidal curves for metal activation, since metals can randomly bind to protein or other biomolecules leading to similarly shaped activation curves. Fourth are experimental plots that show no activation with increasing metal concentrations. This case refers to metals that are incapable of catalyzing the hydrolysis of ATP or that may actually inhibit the reaction. Finally, the second and third kinetic patterns can be combined where a peak velocity is observed, but only if the initial activation curve is sigmoidal.

A. Divalent Metal Activation of Rho in the Absence of $MgCl_2$. The roles of the 11 divalent metals (Be^{2+}, Ca^{2+}, Cd^{2+}, Co^{2+}, Cu^{2+}, Hg^{2+}, Mn^{2+}, Ni^{2+}, Sr^{2+}, VO^{2+}, Zn^{2+}) were investigated in rho-dependent processes and then compared with Mg^{2+}, the metal cofactor. For each metal, we pretreated wild-type rho with 20 mM EDTA to deplete the protein of residual metals and removed the excess EDTA and the metal·EDTA complex by a spin column (*11*). We determined that rho retained 15% or less of residual poly(C)-dependent ATPase activity, and upon addition of 10 mM $MgCl_2$, ∼90% activity of the untreated sample was recovered. The rates of ATP hydrolysis were measured at 12 divalent metal ion concentrations (1.9, 3.8, 7.8, 15.6, 31.3, 62.5, 125, 250, 500, 1000, 2000, 4000 μM), and the residual (≤15%) ATPase activity from the spin column treated rho was subtracted from the observed activity.

Our results show that the divalent metals can be grouped into four classes based on their metal activation profiles. First, Mg^{2+}, Ca^{2+}, Co^{2+}, Cu^{2+}, Hg^{2+}, and VO^{2+} exhibited Michaelis−Menten kinetics. Cd^{2+}, Mn^{2+}, and Zn^{2+} fall in the second group showing peak velocities at different metal concentrations. Within this category, we found that Cd^{2+} and Zn^{2+} showed curves with sigmoidal behavior. The third group contained only Ni^{2+}, which showed a sigmoidal activation pattern rising to a constant V_{max} at high metal concentrations.

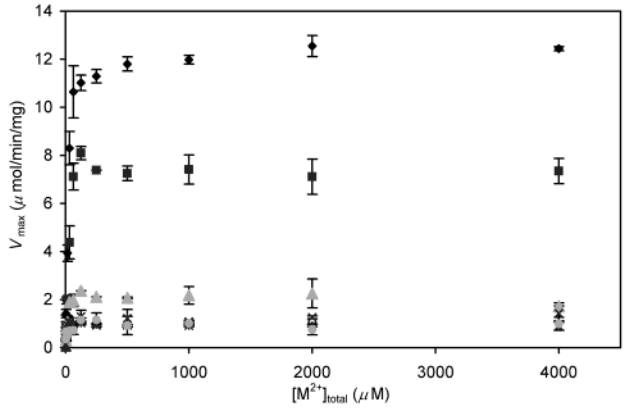

FIGURE 1: Metal activation of rho exhibiting a hyberbolic curve. The reactions were conducted using a solution (100 μL) containing ATPase buffer, rho (100 nM (monomer)), poly(C) (100 nM), ATP (200 μM), and various concentrations of total M^{2+} at 32 °C. The average velocities of two determinations are plotted with Mg^{2+} (◆), Co^{2+} (■), Ca^{2+} (gray triangles), Cu^{2+} (×), Hg^{2+} (*), and VO^{2+} (gray circles).

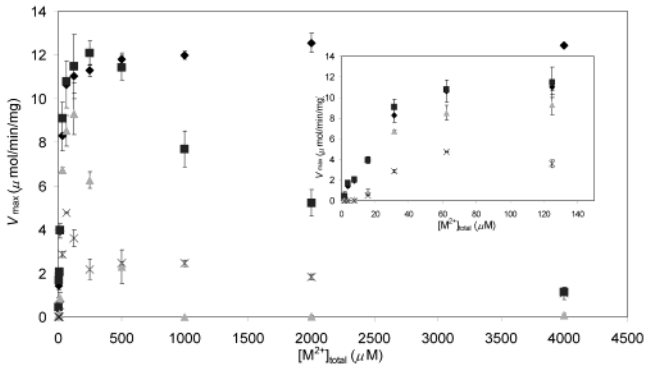

FIGURE 2: Metal activation of rho exhibiting a peak velocity. The reactions were conducted using a solution (100 μL) containing ATPase buffer, rho (100 nM (monomer)), poly(C) (100 nM), ATP (200 μM), and various concentrations of total M^{2+} at 32 °C. The average velocities of two determinations are plotted with Mg^{2+} (◆), Mn^{2+} (■), Zn^{2+} (gray triangles), and Cd^{2+} (×). Inset: metal activation of rho exhibiting a peak velocity and sigmoidal behavior at rho divalent metal concentrations.

Be^{2+} and Sr^{2+} lie in the fourth group and did not catalyze ATP hydrolysis, and thus no activation profiles were observed.

For the first group, maximal ATP hydrolysis rates were observed at metal concentrations of 250 μM and higher, and the order of activation was $Mg^{2+} > Co^{2+} > Ca^{2+} > Cu^{2+} \sim Hg^{2+} \sim VO^{2+}$. Within this group, the best activator, Mg^{2+}, hydrolyzed ATP nearly 10 times faster than the three poorest activators, Cu^{2+}, Hg^{2+}, and VO^{2+}.

Three metals, Cd^{2+}, Mn^{2+}, and Zn^{2+}, showed peak velocities when concentrations were progressively increased from 1.9 to 4000 μM (Figure 2). The Mg^{2+} activation curve is included in the figure for comparison. The peak velocity for Mn^{2+} (11.9 μmol/min/mg) was observed at 250 μM, and the V_{peak} was found to be similar to the Mg^{2+} V_{max}, making both metals equally effective in hydrolyzing ATP at low metal concentrations. Above 250 μM $[Mn^{2+}]_{total}$ the velocity rapidly diminished, reaching 10% of maximum activity at 4000 μM. The peak velocity of Zn^{2+} was 9.4 μmol/min/mg at a $[Zn^{2+}]_{total}$ of 125 μM and then decreased to zero at 1000 μM. We observed a hyperbolic loss in rho activity beyond 125 μM $[Zn^{2+}]_{total}$, and at 190 μM $[Zn^{2+}]_{total}$ only 50% of the activity remained. The hyperbolic drop of the $ZnCl_2$ curve beyond the peak velocity suggested that inhibition occurred by the divalent metal binding to a specific site. Finally, for Cd^{2+} the peak velocity of 4.8 μmol/min/mg was reached at 65 μM $[Cd^{2+}]_{total}$ and slowly tapered off over the higher concentration range. Cd^{2+} and Zn^{2+} exhibited a sigmoidal shape in the hydrolysis rate at low metal concentrations.

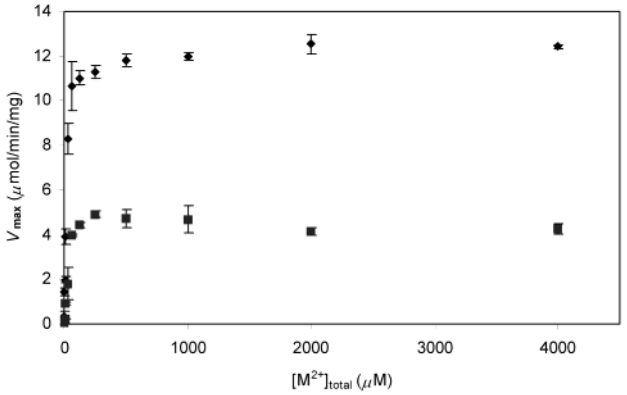

FIGURE 3: Metal activation of Mg^{2+} and Ni^{2+}. The reactions were conducted using a solution (100 μL) containing ATPase buffer, rho (100 nM (monomer)), poly(C) (100 nM), ATP (200 μM), and various concentrations of total M^{2+} at 32 °C. The average velocities of two determinations are plotted with Mg^{2+} (◆) and Ni^{2+} (■).

Preliminary experiments with $MnCl_2$ showed that adding 10 mM $MnCl_2$ to the poly(C)-dependent ATPase assay mixture led to the precipitation of a colorless solid. The presence of poly(C) caused the precipitate, which increased with Mn^{2+} concentration, and the precipitate contained rho (SDS−PAGE analysis, data not shown). We concluded that the precipitate was a Mn^{2+}−poly(C)−rho complex. Support for this notion comes from the report that Mn^{2+} complexes with poly(C) and leads to an increase in the helicity of the homopolymer and precipitation of the coiled complex (*23*). We have attributed the loss of ATPase activity for Mn^{2+} after the observed peak velocity to the formation of this precipitate. No precipitates were observed for the two other metals, Cd^{2+} and Zn^{2+}, which showed peak velocity (data not shown), indicating that the factors contributing to these peak velocities differed from Mn^{2+}.

Ni^{2+} was the only divalent metal studied that showed sigmoidal rate acceleration at low metal concentrations plateauing at a constant V_{max} at high metal concentrations (Figure 3).

Two metals—$Be^{2+}$and Sr^{2+}—showed no activity in the poly(C)-dependent ATPase assay when tested between 0 and 4000 μM total metal concentration.

In Table 1, we summarize the dissociation constant (K_D) for each M·ATP complex at 25 °C (*24*−*26*) along with the observed maximal velocities for each metal, the $K_{M(app)}$, and the Hill constants for the velocity curves, and we calculate the V_{max}/K_M and V_{peak}/K_M values. These numbers are a measure of the efficiency of each metal in rho-mediated ATP hydrolysis. The larger the V/K_M value, the more efficient the enzyme in hydrolyzing ATP.

No correlation was observed in either the maximal velocity for ATP hydrolysis (V_{max} or V_{peak}) or the efficiency of ATP hydrolysis (V/K_M) values with the K_D for the $M{\cdot}ATP^{2-}$ complex. Of the three metals that bound ATP the most tightly (VO^{2+}, Cu^{2+}, Ni^{2+}), only Ni^{2+} gave significant ATP hy-

Table 1: Summary of the Divalent Metals for Rho Activation

M^{2+}	K_D (MATP)[a] (μM)	$V_{max(app)}$[b] (μmol min^{-1} mg^{-1})	$V_{peak(app)}$[b] (μmol min^{-1} mg^{-1})	$K_{M(app)}$[c] (μM)	$V/K_{M(app)}$[d] ($\times 10^3$ min^{-1})	n (Hill)[e]
Mg^{2+}	60.2	12.3	−/−	21.2	579	1
Be^{2+}	−/−	0.21	−/−	n.d.[f]	n.d.	n.d.
Ca^{2+}	107	3.13	−/−	7.3	428	1
Cd^{2+}	43.6	−/−	4.74	41.8	114	4.6
Co^{2+}	21.9	7.65	−/−	21.8	351	1
Cu^{2+}	0.7	1.54	−/−	6.8	227	1
Hg^{2+}	−/−	0.78	−/−	4.7	167	1
Mn^{2+}	16.6	−/−	11.9	23.1	513	1
Ni^{2+}	9.5	4.79	−/−	28.2	170	2.9
Sr^{2+}	288	0.17	−/−	n.d.	n.d.	1
VO^{2+}	0.2	0.78	−/−	n.d.	n.d.	1
Zn^{2+}	14.1	−/−	9.98	33.6	297	5.5
none	−/−	0.70	−/−	n.d.	n.d.	n.d.

[a] K_D(MATP) = [M^{2+}]·[ATP]/[MATP] at 25 °C for Mg^{2+} (*24*), Mn^{2+} (*24*), Zn^{2+} (*24*), Ni^{2+} (*24*), Cd^{2+} (*24*), Ca^{2+} (*24*), Co^{2+} (*24*), Cu^{2+} (*25*), VO^{2+} (*26*), Sr^{2+} (*24*). [b] V_{max} or V_{peak} were determined from the activation curves. [c] K_M determined by estimating total M^{2+} concentration at 0.5·V_{max} or 0.5·V_{peak}. [d] V/K_M is a measure for substrate specificity and efficiency. [e] The Hill constant was determined through nonlinear regressional analysis (SigmaPlot 2001). [f] n.d. = not determined because the values were too low to be accurately calculated.

drolysis. Correspondingly, metals that bound ATP poorly displayed excellent (Mg^{2+}), moderate (Cd^{2+}), weak (Ca^{2+}), or low (Sr^{2+}) velocities for ATP hydrolysis. The $K_{M(app)}$ values for the M·ATP^{2-} substrates were not diagnostic of metal efficiency (V/K_M). The $K_{M(app)}$ for Mg^{2+}, Mn^{2+}, and Co^{2+} were comparable; yet the efficiencies (V_{max}/K_M or V_{peak}/K_M) for Mg^{2+} and Mn^{2+} were 1.5 and 1.6 times that of Co^{2+}, respectively. Finally, inspection of the composite table showed only two possible periodic trends. These were for the series Mg^{2+}, Ca^{2+}, Sr^{2+} (group 2A) and Zn^{2+}, Cd^{2+}, Hg^{2+} (group 2B). The group 2A metals all showed Michaelis−Menten kinetics. Furthermore, we observed a steady drop in the V_{max} and V_{max}/K_M as we progressed down the group. A similar drop in the V_{peak} (V_{max}) and the V_{peak}/K_M (V_{max}/K_M) was observed for the group 2B metals as we proceeded to metals with higher atomic numbers. The only exception in the group 2A metals was Be^{2+}, which produced no rho poly(C)-dependent activity. We attributed this anomaly to the formation of an ATP inhibitory transition state complex upon binding to ADP (see Results, section B) (*27*−*29*). A nonlinear regression analysis program (SigmaPlot2001) was used to determine the Hill coefficients, *n*, seen as the final column in Table 1. Mg^{2+}, Ca^{2+}, Co^{2+}, Hg^{2+}, Mn^{2+}, Sr^{2+}, and VO^{2+} showed a Hill coefficient of 1, while for Cd^{2+}, Ni^{2+}, and Zn^{2+} *n* ranged from 2.9 (Ni^{2+}) to 5.5 (Zn^{2+}). The sigmoidal curves for Zn^{2+}, Cd^{2+}, and Ni^{2+} may signify cooperative behavior; however, they may also suggest additional binding sites on either poly(C) or rho. Thus, we view the Hill constants for these metals with caution and have not associated a specific process to them.

The 12 divalent metals were classified by their maximal rates (V_{max} or V_{peak}) (Figure 4A) and their efficiencies (V_{max}/K_M or V_{peak}/K_M) (Figure 4B) for ATP hydrolysis (Table 2). Using either of these two classification systems, Mg^{2+} and Mn^{2+} were found the best activators in the poly(C)-dependent ATPase assay. It was significant that Ca^{2+}, which was a weak activator based on its V_{max} alone, was the third most efficient metal (V_{max}/K_M) for ATP hydrolysis.

Bicyclomycin (**1**) is the only known natural product that selectively inhibits rho. We have demonstrated that **1** interferes with RNA binding at the secondary site in rho (*30*) and disrupts the nonessential Mg^{2+} activation process required for maximal ATP hydrolysis (*11*). Our studies have

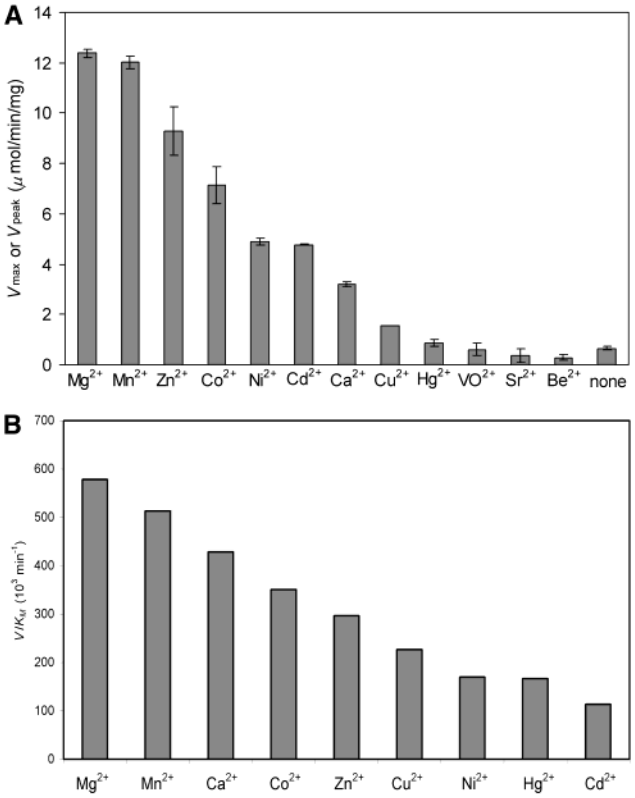

FIGURE 4: A: Maximal velocity for the divalent metals. The velocities displayed are at either their V_{max} or V_{peak} as derived from their activation curve. See captions of Figures 1−3. B: Efficiency of the divalent metals. Listed are the metals V_{max}/K_M or V_{peak}/K_M values vs metal as described in Table 1. The V/K_M values for VO^{2+}, Sr^{2+}, and Be^{2+} could not be determined.

shown that divalent metal ions other than Mg^{2+} can catalyze rho poly(C)-dependent ATP hydrolysis. We then asked whether **1** inhibition was metal specific and focused on Mn^{2+} and Zn^{2+} (Figure 5). Both metals showed peak velocities in their ATP hydrolysis rates (Figure 2). Accordingly, the metal concentrations employed (Mn^{2+}, 200 μM; Zn^{2+}, 100 μM) were below the amount found to give maximal hydrolysis rates. The effect of **1** in the rho poly(C)-dependent ATP activity assay was determined at five inhibitor concentrations (25, 50, 100, 200, 400 μM) and compared with the Mg^{2+}-activated (200 μM) rho sample. We observed similar I_{50}

Table 2: Effect of Metals on Rho Activity[a]

	Mg^{2+}-free		
metal	% activity (V_{max} or V_{peak})	% efficiency (V_{max}/K_M or V_{peak}/K_M)	10 mM $MgCl_2$
Mg^{2+}	100 (e)	100 (e)	n.d.
Be^{2+}	2 (i)	n.d.	i
Ca^{2+}	25 (w)	74 (g)	n
Cd^{2+}	39 (m)	20 (w)	n
Co^{2+}	62 (g)	61 (g)	n
Cu^{2+}	13 (p)	39 (m)	i
Hg^{2+}	6 (p)	29 (w)	i
Mn^{2+}	97 (e)	89 (e)	n.d.
Ni^{2+}	39 (m)	29 (w)	n
Sr^{2+}	1 (n)	n.d.	n
VO^{2+}	6 (p)	n.d.	n
Zn^{2+}	81 (g)	51 (m)	i

[a] e = excellent activator; g = good activator; m = moderate activator; w = weak activator; p = poor activator; n = nonactivating metal; i = inhibitor; n.d. = not determined.

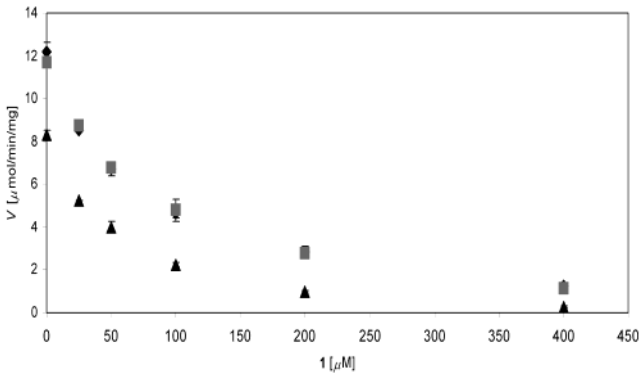

FIGURE 5: Bicyclomycin inhibition of divalent metal-mediated rho poly(C)-dependent ATP hydrolysis. The reactions were conducted using a solution (100 μL) containing ATPase buffer, rho (100 nM (monomer)), poly(C) (100 nM), ATP (200 μM), and either total $MgCl_2$ (200 μM) (◆), total $MnCl_2$ (200 μM) (gray squares), or total $ZnCl_2$ (100 μM) (▲) and bicyclomycin as indicated at 32 °C. The average of two determinations are plotted. The observed V_{max} ([**1**] = 0 μM) at the given metal concentrations were 12.2, 11.7, and 8.3 μmol min^{-1} mg^{-1} for Mg^{2+}, Mn^{2+}, and Zn^{2+}, respectively.

values for **1** (50−60 μM) in all three metals. These results indicated that the inhibitory activity for **1** in the poly(C)-dependent ATPase assay was not affected by the decrease of the Mg^{2+} concentration from the standard condition of 12 mM (*31*) to 200 μM and that the I_{50} for **1** did not change when either Mn^{2+} or Zn^{2+} was employed as the activating metal.

B. Divalent Metal Activation of Rho in the Presence of $MgCl_2$. To provide additional information concerning the roles of divalent metals in rho activation, we repeated the poly(C)-dependent assays in the presence of 10 mM $MgCl_2$ and varying concentrations (10, 20, 40, 80, 125, 160, 250, 320, 500, 640 μM) of the divalent metals. We chose Be^{2+}, Ca^{2+}, Cd^{2+}, Co^{2+}, Hg^{2+}, Ni^{2+}, Sr^{2+}, VO^{2+}, and Zn^{2+} and excluded Mn^{2+} from this study since $MnCl_2$ precipitated the poly(C)-rho complex.

Ni^{2+}, Ca^{2+}, Cd^{2+}, Co^{2+}, VO^{2+}, and Sr^{2} had negligible effects on ATP hydrolysis rate in the presence of $MgCl_2$ (Supporting Information, Figure 1). This finding indicated that at 10 mM $MgCl_2$, Mg^{2+} can effectively compete with these metals for the essential sites in rho necessary for ATP hydrolysis and that these metals do not adversely interact with rho, ATP, ADP, and poly(C). Included in this list was Sr^{2+}, a metal previously identified as either a nonactivator or an inhibitor. The lack of inhibition by Sr^{2+} in the presence of $MgCl_2$ indicated that this metal did not inactivate rho under these conditions, and thus is a nonactivator.

Four divalent metal ions (Be^{2+}, Cu^{2+}, Hg^{2+}, Zn^{2+}) inhibited rho poly(C)-dependent ATP hydrolysis in the presence of $MgCl_2$ (10 mM) (Supporting Information, Figure 2). The extent and pattern of inhibition was metal dependent. Cu^{2+} caused a modest loss of activity (~30%), while larger decreases in activities were noted for Hg^{2+} and Zn^{2+}. At 4000 μM Hg^{2+} and Zn^{2+}, rho inhibition was ~50%. Nonhyperbolic inactivation curves were observed for Cu^{2+}, Hg^{2+}, and Zn^{2+}, suggesting that rho inhibition proceeded, in part, by a nonselective process and $ZnCl_2$ inhibition was found to be dependent on the $MgCl_2$ concentration. The estimated I_{50} values for $ZnCl_2$ were 190, 190, and 4000 μM in the presence of 0, 1, and 10 mM $MgCl_2$, respectively (Supporting Information, Figure 3). Furthermore, the I_{50} value for $ZnCl_2$ increased only slightly when the poly(C) concentration was increased 10-fold (Supporting Information, Figure 4). These findings indicated that the Zn^{2+} inhibition process was partially prevented by excess Mg^{2+} and that Zn^{2+} inhibition did not occur by RNA complexation. Of the 10 metals tested with 10 mM $MgCl_2$, only $BeCl_2$ showed a clear inhibition curve with an I_{50} value of 63 μM (Supporting Information, Figure 2). At 100 μM $BeCl_2$ we observed almost complete loss of activity. Why Be^{2+}? Previous studies have shown that BeX_y (X = F, Cl; y = 2, 3) can bind with ADP to generate an ATP transition state complex that resembles ATP and inhibits ATP-dependent processes (*27*−*29*). We suspect that a similar process occurred in our experiments when the newly generated ADP bound with $BeCl_2$ in solution.

DISCUSSION

We have investigated the metal dependency for rho activation. Lowery and Richardson also reported the Mg^{2+}, Ca^{2+}, Cd^{2+}, Co^{2+}, Cu^{2+}, Mn^{2+}, and Zn^{2+} dependency for rho activation in the poly(C)-dependent ATPase assay (*10*). They classified these metals into three groups: Mg^{2+} and Mn^{2+} were termed rho ATPase activators, Ca^{2+}, Co^{2+}, and Cu^{2+} were classified as slight inhibitors, and Cd^{2+} and Zn^{2+} were found to be potent inhibitors. We first removed over 85% of the rho-bound Mg^{2+} by treatment with EDTA followed by size-exclusion chromatography (*11*). No DTT was added to the incubation and assay buffers because DTT is known to bind metals (*32*, *33*). The metals tested in the Lowery and Richardson study were used, and their list was expanded to include Be^{2+}, Hg^{2+}, Ni^{2+}, Sr^{2+}, and VO^{2+}. Many of the tested divalent metals were found to activate rho, but the rate of rho activation was dependent upon the metal and its concentration.

Our classification for divalent metals was different than that reported by Lowery and Richardson (*10*). Table 2 summarizes the effect of the 11 divalent metals in the rho poly(C)-dependent ATP assay on the observed velocity (V_{max}, V_{peak}) and efficiency (V_{max}/K_M, V_{peak}/K_M) in the absence and the presence of 10 mM $MgCl_2$. On the basis of the observed velocity (V_{max}, V_{peak}), Mg^{2+} and Mn^{2+} were the most effective, followed by Zn^{2+} and Co^{2+} (good activators), Ni^{2+} and

Cd^{2+} (moderate activators), Ca^{2+} (a weak activator), and Cu^{2+}, Hg^{2+}, and VO^{2+} (poor activators). On the basis of efficiency (V_{max}/K_M, V_{peak}/K_M), Mg^{2+} and Mn^{2+} again were the most effective metals, followed by Ca^{2+} and Co^{2+} (good activators) and Cu^{2+} (moderate activator). The rank order for the good, moderate, and weak activators differed between the two classification systems. In particular, we observed that when the metals were ranked in terms of efficiency rather than velocity, Ca^{2+}, Cu^{2+}, and Hg^{2+} were classified as better activators, and Cd^{2+}, Ni^{2+}, and Zn^{2+} were ranked as poorer activators. Of these rank order changes, Ca^{2+} was the most dramatic, being classified as the third most efficient divalent metal in this assay although its velocity was only 25% that of Mg^{2+}. The change in classification is due, in part, to the apparent K_M value for Ca·ATP^{2-} ($K_{M(app)} = 7.3\ \mu M$). This value was nearly three times lower than the Mg·ATP^{2-} ($K_{M(app)} = 21.2\ \mu M$), indicating that rho has a higher affinity for Ca·ATP^{2-} than for Mg·ATP^{2-}.

We have found Cd^{2+} and Zn^{2+} to be significant rho activators at low metal concentrations, while Lowery and Richardson reported that these divalent metals to be potent inhibitors. Why? The divalent metal concentration is part of the answer. We used metal concentrations that spanned 0−4 mM, while in the Lowery and Richardson investigation the metal concentration was 1 mM. This difference explains, in part, the result why $ZnCl_2$ was previously termed an inactivator. We, too, found 1 mM $ZnCl_2$ to be an inactivator. However, we observed that $ZnCl_2$ was a significant activator at concentrations below 125 μM. The effect of metal concentration on rho activity did not explain why we observed 1 mM $CdCl_2$ to be an activator and Lowery and Richardson classified it as a potent inhibitor. The different findings have been traced to the DL-DTT present in the buffer solutions employed in the Lowry and Richardson study. We will report in a future paper our findings about the potent rho inhibitory activities of metal·DTT and metal·thiol chelates.

The effect of bicyclomycin was independent of the nature of the metal. Replacement of $MgCl_2$ (200 mM) in the poly(C)-dependent assay by either $MnCl_2$ or $ZnCl_2$ had no appreciable effect on the inhibitory activity of **1** (Figure 5). We have reported that bicyclomycin disrupted RNA binding to the secondary site in rho (*30*) and interfered with the nonessential Mg^{2+} activation pathway for rho ATP hydrolysis (*11*). The near equivalent **1** I_{50} values for Mg^{2+}-, Mn^{2+}-, and Zn^{2+}-initiated processes demonstrated that the antibiotic inhibition pathway was metal independent.

Recent studies have drawn attention to the close structural similarly of rho with the β-subunit in F_1-ATP synthase (*34*−*38*). Studies by Walker (*39*) and Senior (*40*) have demonstrated that Mg^{2+} ligation at the Mg·ATP^{2-} binding site in the β-subunit of F_1-ATP synthase proceeds by direct coordination to βThr156 and through bridging water molecules by hydrogen bonds to βGlu185 and βAsp242 (Figure 6A). The remaining positions in the octahedron around the Mg^{2+} ion in F_1-ATP synthase are occupied by the ATP β- and γ-phosphate oxygens. Senior and co-workers have further proposed that Mg·ATP^{2-} hydrolysis proceeds by an in-line nucleophilic mechanism where the aligned water, which displaces the γ-phosphate in Mg·ATP (*40*, *41*), is aided by βGlu181. Sequence comparison of all these residues to *E. coli* rho showed that they are conserved (Figure 6B) and are properly positioned in our model to bind to ATP (Mg·ATP^{2-}). Our study showed that rho activity was not specific for the octahedral metal Mg^{2+} and that the other six coordinate metals, such as Mn^{2+} and Ca^{2+}, can catalyze ATP hydrolysis. Moreover, we found that the efficiency (V_{max}/K_M or V_{peak}/K_M) of Mn^{2+} was 89% that of Mg^{2+} and Ca^{2+} was 74% of Mg^{2+} (Table 2), suggesting that these divalent metal ions can effectively bind to the rho ATP hydrolysis pocket. Interestingly, we found that rho can be activated by metals that often prefer coordination spheres less than six (*42*). The five-coordinate (trigonal bipyramidal, square pyramidal) metals Co^{2+}, Ni^{2+}, and VO^{2+} activated rho. The rates (V_{max}, V_{peak}) for these three metals were 6−61% of Mg^{2+} at 4000 μM, and Co^{2+} was found to be 61% as efficient (V_{max}/K_M) as Mg^{2+} (Table 2). Similarly, the four coordinating cations Zn^{2+} and Cd^{2+} were among the most effective metals in the poly(C)-dependent assay. At 125 μM Zn^{2+}, the rate of ATP hydrolysis was 81% of that observed for Mg^{2+}, making this divalent metal 51% as efficient as Mg^{2+} (Table 2). Our finding that metals, which are generally tetra- and penta-ligated, were effective activators in the poly(C)-dependent ATP assay suggested that conservation of the putative Mg·ATP^{2-} coordination sphere in rho need not remain fully intact for ATP hydrolysis.

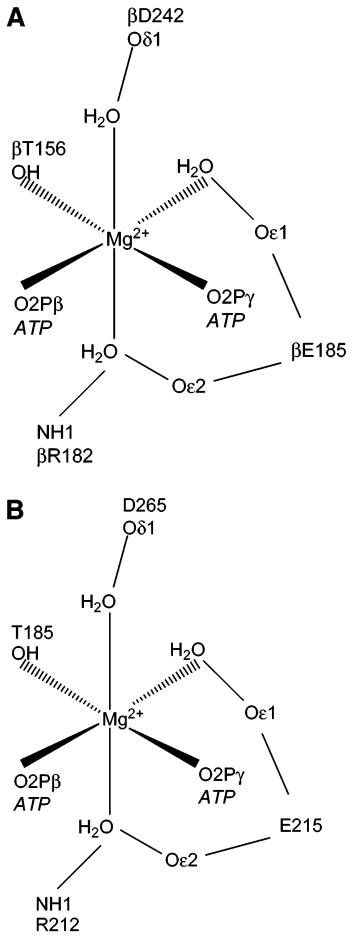

FIGURE 6: A: MgATP binding site in F_1-ATP synthase. Octahedral coordination of Mg^{2+} in F_1-ATP synthase (*40*). B: MgATP binding site in rho. Projected octahedral coordination of Mg^{2+} for rho based on F_1-ATP synthase.

CONCLUSIONS

Mg^{2+} is essential for rho-dependent functions and without it ATP hydrolysis does not occur and rho-dependent transcription termination ceases. We learned that many divalent metals support ATP hydrolysis in the rho poly(C)-dependent ATPase assay, suggesting that flexibility exists in the coordination sphere in rho for metal binding and catalysis.

ACKNOWLEDGMENT

We thank Dr. M. Kawamura and the Fujisawa Pharmaceutical Co., Ltd., Japan, for the gift of bicyclomycin and Dr. T. Platt (University of Rochester) for the overproducing strain of rho.

SUPPORTING INFORMATION AVAILABLE

Divalent metal activation profiles for the poly(C)-dependent assay run in the presence of excess of $MgCl_2$. This material is available free of charge via the Internet at http://pubs.acs.org.

REFERENCES

1. Roberts, J. W. (1969) Termination factor for RNA synthesis, *Nature 224*, 1169−1174.
2. Pinkham, J. L., and Platt, T. (1983) The nucleotide sequence of the *rho* gene of *E. coli* K-12, *Nucleic Acids Res. 11*, 3531−3545.
3. Richardson, J. P. (1990) Rho-dependent transcription termination, *Biochim. Biophys. Acta 1048*, 127−138.
4. Platt, T., and Richardson, J. P. (1992) in *Transcriptional Regulation* (McKnight, S. L., and Yamamoto, K. R., Eds.) pp 365−388, Cold Spring Harbor Laboratory Press, Plainview, NY.
5. Das, A., Court, D., and Adhya, S. (1976) Isolation and characterization of conditional lethal mutants of *Escherichia coli* defective in transcription termination factor rho, *Proc. Natl. Acad. Sci. U.S.A. 73*, 1959−1963.
6. Inoko, H., Shigesda, K. and Imai, M. (1977) Isolation and characterization of conditional-lethal rho mutants of *Escherichia coli*, *Proc. Natl. Acad. Sci. U.S.A. 74*, 1162−1166.
7. Richardson, J. P., and Carey, J. L., III. (1982) Rho factors from polarity suppressor mutants with defects in their RNA interactions, *J. Biol. Chem. 257*, 5767−5771.
8. Russel, M., and Model, P. (1984) Replacement of the fip gene of *Escherichia coli* by an inactive gene cloned on a plasmid, *J. Bacteriol. 159*, 1034−1039.
9. Stitt, B. L. (1988) *Escherichia coli* transcription termination protein rho has three hydrolytic sites for ATP, *J. Biol. Chem. 263*, 11130−11137.
10. Lowery, C., and Richardson, J. P. (1977) Characterization of the nucleoside triphosphate phosphohydrolase (ATPase) activity of RNA synthesis termination factor *ρ*. I. Enzymatic properties and effects of inhibitors, *J. Biol. Chem. 252*, 1375−1380.
11. Weber, T. P., Widger, W. R., and Kohn, H. (2002) The Mg^{2+} requirements for rho transcription termination factor: catalysis and bicyclomycin inhibition, *Biochemistry 41*, 12377−12383.
12. Mildvan, A. S. (1987) Role of magnesium and other divalent cations in ATP-utilizing enzymes, *Magnesium 6*, 28−33.
13. Syroeshkin, A. V., Galkin, M. A., Sedlov, A. V., and Vinogradov, A. D. (1999) Kinetic mechanism of F_0•F_1 mitochondrial ATPase: Mg^{2+} requirement for Mg•ATP hydrolysis, *Biochemistry (Moscow) 64*, 1128−1337.
14. Davies, P. L., and Bragg, P. D. (1972) Properties of a soluble Ca^{2+}- and Mg^{2+}-activated ATPase released from *Escherichia coli* membranes, *Biochim. Biophys Acta 266*, 273−284.
15. Schobert, B. (1992) The binding of a second divalent metal ion is necessary for the activation of ATP hydrolysis and its inhibition by tightly bound ADP in the ATPase from *Halobacterium saccharovorum*, *J. Biol. Chem. 267*, 10252−10257.
16. Hicks, D. B., and Krulwich, T. A. (1987) Purification and characterization of the F_1 ATPase from *Bacillus subtills* and its uncoupler-resistant mutant derivatives, *J. Bacteriol. 169*, 4743−4749.
17. Veltrup, W. (1981) Effect of heavy metals on the [activity of] ATPases, *Ber. Dtsch. Bot. Ges. 93*, 659−666.
18. Mott, J. E., Grant, R. A., Ho, Y.-S., and Platt, T. (1985) Maximizing gene expression from plasmid vectors containing the λP_L promoter: Strategies for overproducing transcription termination factor *ρ*, *Proc. Natl. Acad. Sci. U.S.A. 82*, 88−92.
19. Nehrke, K. W., Seifried, S. E., and Platt, T. (1992) Overproduced rho factor from p39AS has lysine replacing glutamic acid at residue 155 in the linker region between its RNA and ATP binding domains, *Nucleic Acids Res. 20*, 6107.
20. Lowry, O. H., Rosebrough, N. J., Farr, A. L., and Randall, R. J. (1951) Protein measurement with the folin phenol reagent, *J. Biol. Chem. 193*, 265−275.
21. Sharp, J. A., Galloway, J. L., and Platt, T. (1983) A kinetic mechanism for the poly(C)-dependent ATPase of the *Escherichia coli* transcription termination protein, rho, *J. Biol. Chem. 258*, 3482−3486.
22. London, W. P., and Steck, T. L. (1969) Kinetics of enzyme reactions with interaction between a substrate and a (metal) modifier, *Biochemistry 8*, 1767−1779.
23. Sorokin, V. A., Blagoi, Y. P., Valeev, V. A., Gladchenko, G. O., Sindelkova, E. and Savin, F. A. (1986) Spectroscopic studies of bivalent metal ion binding to single-stranded polyC, *Stud. Biophys. 114*, 269−276.
24. Khan, M. M. T., and Martell, A. E. (1966) Thermodynamic quantities associated with the interaction of adenosine triphosphate with metal ions, *J. Am. Chem. Soc. 88*, 668−671.
25. Pecoraro, V. L., Hermes, J. D., and Cleland, W. W. (1984) Stability constants of magnesium and cadmium complexes of adenine nucleotides and thionucleotides and rate constants for formation of dissociation of magnesium-ATP and magnesium-ADP, *Biochemistry, 23*, 5262−5271.
26. Cini, R., Giorgi, G., Laschi, F., Sabat, M., Sabatini, A., and Vacca, A. (1989) Potentiometric and electron spin resonance investigation on the interactions between adenosine 5′-triphosphate (ATP) and triphosphate ligands with vanadyl ion. Synthesis and characterization of solid vanadyl-ATP compounds from acidic aqueous solution, *J. Chem. Soc., Dalton Trans.* 575−580.
27. Kanfer, J. N., and McCartney, D. (1994) Phospholipase D activity of isolated rat brain plasma membranes, *FEBS Lett. 337*, 251−254.
28. Toda, G., Koie, H., and Yoshitoshi, Y. (1971) Effects of cations on the inhibition of K^+-activated phosphatase by beryllium, *J. Biochem. 69*, 73−82.
29. Santacroce, G., and Costabile, F. (1966) Inhibition of alkaline phosphatase by beryllium chloride in a continuous cellular line of mouse embryonic liver cells, *Boll.-Soc. Ital. Biol. Sper. 42*, 1023−1026.
30. Magyar, A., Zhang, X., Kohn, H., and Widger, W. R. (1996) The antibiotic bicyclomycin affects the secondary RNA binding site of *Escherichia coli* transcription termination factor rho, *J. Biol. Chem. 271*, 25369−25374.
31. Park, H.-g., Zhang, X., Moon, H.-s., Zwiefka, A., Cox, K., Gaskell, S. J., Widger, W. R., and Kohn, H. (1995) Bicyclomycin and dihydrobicyclomycin inhibition kinetics of *Escherichia coli* rho-dependent transcription termination factor ATPase activity, *Arch. Biochem. Biophys 323*, 447−454.
32. Lees, W. J.; Singh, R.; and Whitesides, G. M. (1991) meso-2,5-Dimercapto-N, N, N′, N′-tetramethyladipamide: a readily available, kinetic rapid reagent for the reduction of disulfides in aqueous solution, *J. Org. Chem. 56*, 7328−7331.
33. Krezel, A., Lesniak, W., Jezowska-Bojczuk, M., Mlynarz, P., Brasun, J., Kozlowski, H., and Bal, W. (2001) Coordination of heavy metals by dithiothreitol, a commonly used thiol group protectant, *J. Inorg. Biochem. 84*, 77−88.
34. Horiguchi, T., Miwa, Y., and Shigesada, K. (1997) The quaternary geometry of transcription termination factor rho: Assignment by chemical cross-linking, *J. Mol. Biol. 269*, 514−528.
35. Miwa, Y., Horiguchi, T., and Shigesada, K. (1995) Structural and functional dissections of transcription termination factor Rho by random mutagenesis, *J. Mol. Biol. 254*, 815−837.
36. Richardson, J. P. (1996) Structural organization of transcription termination factor Rho, *J. Biol. Chem. 271*, 1251−1254.

37. Magyar, A., Zhang, X., Abdi, F., Kohn, H., and Widger, W. R. (1999) Identifying the bicyclomycin binding domain through biochemical analysis of antibiotic-resistant rho proteins, *J. Biol. Chem. 274*, 7316−7324.
38. Vincent, F., Openshaw, M., Trautwein, M., Gaskell, S. J., Kohn, H., and Widger, W. R. (2000) Rho transcription factor: Symmetry and binding of bicyclomycin, *Biochemistry 39*, 9077−9083.
39. Abrahams, J. P., Leslie, A. G., Lutter, R., and Walker, J. E. (1994) Structure at 2.8 Å resolution of F_1-ATPase from bovine heart mitochondria, *Nature 370*, 621−628.
40. Weber, J., Hammond, S. T., Wilke-Mounts, S., Senior, A. E. (1998) Mg^{2+} coordination in catalytic sites of F_1-ATPase, *Biochemistry 37*, 608−614.
41. Weber, J., Nadanaciva, S., and Senior, A. E. (2000) ATP-driven rotation of the γ subunit in F_1-ATPase, *FEBS Lett. 483*, 1−5.
42. Douglas, B. and McDaniels, D. (1965) *Concepts and Models of Inorganic Chemistry*, pp 313−315, Blaisdell Publishing Co., Waltham, MA.

BI020601Y